Arch Appl Mech (2015) 85:1499–1511
DOI 10.1007/s00419-014-0947-6

SPECIAL

K. V. Spiliopoulos · K. D. Panagiotou

A numerical procedure for the shakedown analysis of structures under cyclic thermomechanical loading

Received: 27 December 2013 / Accepted: 22 May 2014 / Published online: 25 November 2014

Abstract Determining safety margins for a structure or a component against excessive inelastic deformations is an important issue for engineering design. Direct methods and particularly shakedown analysis constitute a convenient tool towards this direction. Most of the developed approaches in shakedown analysis are based on optimization algorithms. In this paper, a procedure for the shakedown analysis of structures under thermo-mechanical loads is presented. The approach makes use of the recently published Residual Stress Decomposition Method (RSDM) which assumes the decomposition of the residual stress field into Fourier series with respect to time. Starting from a high loading factor, the shakedown limit is estimated through an iterative procedure that updates the Fourier coefficients, reducing at the same time this loading factor until the only remaining term of the Fourier series is the constant term. The method is formulated within the finite element method and is applied to two-dimensional structures under thermal and mechanical cyclic loading.

Keywords Direct methods · Plasticity · Shakedown analysis · Cyclic loading · Limit cycle · Fourier series

1 Introduction

An important task in civil and mechanical engineering is the calculation of the load carrying capacity of a structure or a component under cyclic loadings. Structures like pavements, bridges, nuclear reactors, and aircraft propulsion engines fall into this category. The applied cyclic thermal and mechanical loads often lead the structures beyond the elastic region where plastic straining takes place. In order for a structure to be safe and serviceable, one may produce safety margins like shakedown limits so that the structure fails neither due to incremental collapse nor due to alternating plasticity.

When the exact loading history is known, one may estimate the long- term behavior of a structure using step by step methods which require large computing time. A much better alternative, that requires much less computing time, is offered by the direct methods that may directly predict the cyclic behavior of the structure. These methods do not require the knowledge of the exact lifetime loading history of the structure but only its variation interval.

The ingredient of these methods is the existence of a steady state at the end of the loading procedure for structures made of ductile material [1]. Typical examples of such methods are the limit analysis for monotonic loading and the shakedown analysis for loading varying cyclically. For small displacements and elastic–perfectly plastic solids, the lower bound (Melan [2]) or the upper bound (Koiter [3]) theorems offer ways to

K. V. Spiliopoulos (✉) · K. D. Panagiotou
Department of Civil Engineering, Institute of Structural Analysis and Antiseismic Research, National Technical University of Athens, Zografou Campus, 157-80 Athens, Greece
E-mail: kvspilio@central.ntua.gr

K. D. Panagiotou
E-mail: kdpanag@central.ntua.gr

search for an elastic shakedown state. The extensions of these two theorems to cover thermal loadings were given by Prager [4] and Donato [5], respectively.

Since these works, extensions were made to include other effects like geometric nonlinearities (e.g., [6]), limited linear hardening (e.g., [7]), and nonlinear kinematic hardening (e.g., [8]).

Non-associated plasticity has also been addressed (e.g., [9]). Furthermore, shakedown theorems have also been formulated within the framework of gradient plasticity concepts [10]. Finally, issues concerning dynamic shakedown have also appeared (e.g., [11]).

The numerical approaches towards the solution of the shakedown problem are based on either the lower or the upper bound theorems of plasticity and are cast in the form of mathematical programming (MP) aiming to minimize or maximize an objective function which normally represents the loading factor. Depending on whether the objective function and/or the constraints are linear or nonlinear, the problem can be formulated as a linear (LP) (e.g., [12]) or a nonlinear (NLP) programming problem (e.g., [8]). The discretization of the continuum by a large number of finite elements and the big number of constraints often lead to the solution of large size optimization problems. Various numerical techniques to solve these problems have been developed. Among these, one could mention the reduced basis technique (e.g., [13]) or algorithms based on Newton iterations (e.g., [14]). More recently, a great number of publications have used the interior point algorithms to solve limit and shakedown analysis problems because of their capabilities to solve large scale optimization problems (e.g., [15–21]). Most recent applications of these algorithms to various problems related to either solid or soil mechanics may be found in [22].

One may also find some alternative approaches in the literature for the evaluation of the shakedown load. Such an approach that uses internal variables, with each of them corresponding to an inelastic mechanism, has been developed [23]. A more recent approach, developed on physical, rather than mathematical arguments, is the linear matching method (LMM) [24]. This method is a generalization of the elastic compensation method (e.g., [25]) and is based on matching a linear problem to a plasticity problem. The method constitutes an upper bound approach that generates a sequence of linear solutions, with spatially varying moduli, which converges to the shakedown load of solid mechanics problems (e.g., [26,27]). The method has also been implemented to soil mechanics related to shakedown problems (e.g., [28,29]). The method has been extended beyond shakedown to provide the ratchet boundary for a loading that can be decomposed into constant and time-varying components ([30,31]).

A relatively simple direct method, which was named Residual Stress Decomposition Method (RSDM), was presented recently [32]. The method can predict the long-term cyclic state of an elastic– perfectly plastic structure when subjected to a given cyclic loading history. The approach is also based on physical arguments, and the ground for its development is the expected cyclic nature of the residual stresses. The residual stresses are decomposed into Fourier series with respect to time, and the coefficients of these series are found iteratively by satisfying equilibrium and compatibility at time points inside the cycle. As proved in [32], the method is capable to predict any different cyclic steady state either it is shakedown or alternating plasticity or incremental collapse.

In the present work, a numerical approach for the evaluation of the shakedown load of elasto-plastic structures under cyclic thermo-mechanical loading is presented. Now, only the variation intervals of the loads are known. Nevertheless, the problem may be converted to an equivalent prescribed loading problem by drawing any time curve crossing these intervals. An elastic analysis is performed, and the starting parameters of this loading are evaluated so as the whole structure becomes plastic. This loading is obviously far above shakedown. The proposed procedure generates a sequence of descending loading cyclic solutions through the use of the RSDM. The limit of this sequence is the shakedown loading where the only remaining term in the Fourier series decomposition of the residual stresses field is the constant term. The procedure is applied to a couple of two-dimensional plates under plane stress conditions loaded by thermo-mechanical loading. A von Mises yield surface is assumed to hold.

2 Some theoretical and computational aspects

Let us consider a body of volume V and surface S. Let us assume that the body is subjected to a mechanical load on a part of S, and another part of S has zero displacements. Let us further assume that this loading has the form:

$$P(t) = P(t + nT) \tag{1}$$

Let us further consider that the body (Fig. 1a) is also subjected to some temperature load of the form:

$$\theta(t) = \theta(t + nT), \quad \theta(t) = \theta(x, y, z, t) \tag{2}$$

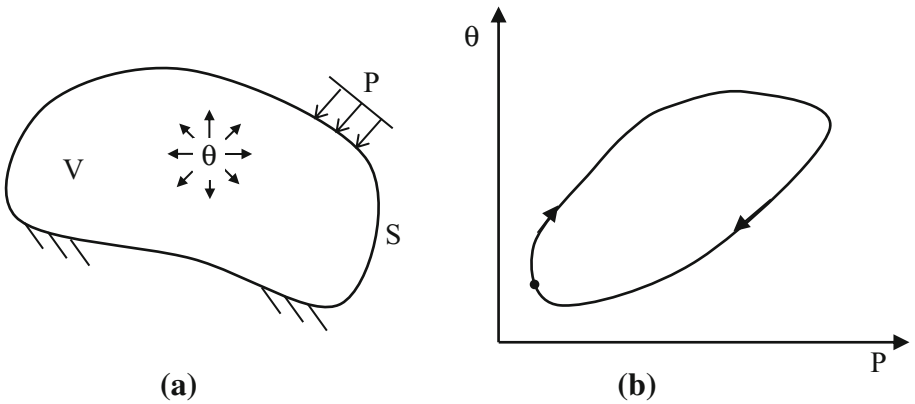

Fig. 1 **a** Structure with applied loads, **b** cyclic loading state

where x, y, z are the spatial coordinates of a point inside the body.

Such a loading constitutes a cyclic loading state having a period T, with t denoting a time point inside a cycle and n being the number of full cycles. A loading trajectory in a two-dimensional loading domain may be seen in Fig. 1b.

For a material exhibiting elasto-plastic behavior, we may assume that at any cycle point $\tau = t/T$ the stress field in the structure may be decomposed into two parts: the first part is $\boldsymbol{\sigma}^{\mathrm{el}}(\tau)$, assuming a purely linear elastic behavior, which may be found to equilibrate the external loading, and a second, self-equilibrating residual stress part $\boldsymbol{\rho}(\tau)$ which is due to inelasticity. One may thus write:

$$\boldsymbol{\sigma}(\tau) = \boldsymbol{\sigma}^{\mathrm{el}}(\tau) + \boldsymbol{\rho}(\tau) \tag{3}$$

where bold letters denote vectors and matrices.

Let us suppose that our structure is discretized, following a standard procedure, into a finite number of elements that are interconnected at a discrete number of nodal points situated on their boundaries.

Considering the linear elastic behavior, we may split the loading into the mechanical and the thermal one. Let us briefly discuss the thermal loading; $\mathbf{r}(\tau)$ denotes the vector of the nodal displacements at some cycle time τ, due to this load. The strains at the Gauss integration points (GPs) may be expressed by (4):

$$\mathbf{e}(\tau) = \mathbf{B}\mathbf{r}(\tau) \tag{4}$$

Assuming some distribution of thermal strains $\mathbf{e}^{\theta}$, an elastic straining is needed so that compatibility is assured:

$$\mathbf{e}(\tau) = \mathbf{e}^{\mathrm{el}}(\tau) + \mathbf{e}^{\theta}(\tau) = \mathbf{D}^{-1}\boldsymbol{\sigma}_{\theta}^{\mathrm{el}}(\tau) + \mathbf{e}^{\theta}(\tau) \tag{5}$$

where $\mathbf{D}$ is the material matrix. Thus, one may write:

$$\boldsymbol{\sigma}_{\theta}^{\mathrm{el}}(\tau) = \mathbf{D}\mathbf{e}(\tau) - \mathbf{D}\mathbf{e}^{\theta}(\tau) \tag{6}$$

Using the principle of virtual work one may write:

$$\int_{\mathrm{V}} \delta\mathbf{e}(\tau)^{\mathrm{T}}\boldsymbol{\sigma}_{\theta}^{\mathrm{el}}(\tau)\mathrm{d}V = 0 \tag{7}$$

since no nodal forces, due to thermal loading develop. Combining (4), (6), and (7), the following expression may be written:

$$\left(\int_{\mathrm{V}} \mathbf{B}^{\mathrm{T}}\mathbf{D}\mathbf{B}\mathrm{d}V\right)\mathbf{r}(\tau) = \int_{\mathrm{V}} \mathbf{B}^{\mathrm{T}}\mathbf{D}\mathbf{e}^{\theta}(\tau)\mathrm{d}V \tag{8}$$

or equivalently:

$$\mathbf{K}\mathbf{r}(\tau) = \int_{\mathrm{V}} \mathbf{B}^{\mathrm{T}}\mathbf{D}\mathbf{e}^{\theta}(\tau)\mathrm{d}V \tag{9}$$

where $\mathbf{K}$ is the stiffness matrix of the structure. Thus, after the solution of (9) for $\mathbf{r}(\tau)$, we may get the values for $\boldsymbol{\sigma}_{\theta}^{\mathrm{el}}(\tau)$ using Eqs. (4) and (6). The corresponding values of the stresses $\boldsymbol{\sigma}_{\mathrm{P}}^{\mathrm{el}}(\tau)$ due to the mechanical loading may be easily obtained, in an analogous way, after the conversion of the loading to the equivalent nodal forces vector $\mathbf{R}(\tau)$, using this vector as the r.h.s of equation (9) and omitting the second part of Eq. (6).

Inelasticity manifests itself through the residual stresses as noted in Eq. (3). An analogous decomposition to this equation holds for the strain rates:

$$\dot{\boldsymbol{\varepsilon}}(\tau) = \dot{\mathbf{e}}(\tau) + \dot{\boldsymbol{\varepsilon}}_{\mathrm{r}}(\tau) \tag{10}$$

where $\dot{\mathbf{e}}(\tau)$ may be evaluated from Eq. (5); $\mathbf{e}^{\mathrm{el}}(\tau)$ will now include elastic straining due to both the thermal and the mechanical loading. The residual strain rate $\dot{\boldsymbol{\varepsilon}}_{\mathrm{r}}(\tau)$ may be itself decomposed into elastic and plastic parts. Thus, Eq. (10) becomes:

$$\dot{\boldsymbol{\varepsilon}}(\tau) = \dot{\mathbf{e}}^{\mathrm{el}}(\tau) + \dot{\mathbf{e}}^{\theta}(\tau) + \dot{\boldsymbol{\varepsilon}}_{\mathrm{r}}^{\mathrm{el}}(\tau) + \dot{\boldsymbol{\varepsilon}}^{\mathrm{pl}}(\tau) \tag{11}$$

Stress rates and elastic strain rates are related by:

$$\begin{aligned} \dot{\boldsymbol{\sigma}}^{\mathrm{el}}(\tau) &= \mathbf{D}\dot{\mathbf{e}}^{\mathrm{el}} \\ \dot{\boldsymbol{\rho}}(\tau) &= \mathbf{D}\dot{\boldsymbol{\varepsilon}}_{\mathrm{r}}^{\mathrm{el}} \end{aligned} \tag{12}$$

Combining Eqs. (11) and (12), we may solve for the rates of the residual stresses:

$$\dot{\boldsymbol{\rho}}(\tau) = \mathbf{D}\dot{\boldsymbol{\varepsilon}}(\tau) - \dot{\boldsymbol{\sigma}}^{\mathrm{el}}(\tau) - \mathbf{D}\dot{\mathbf{e}}^{\theta}(\tau) - \mathbf{D}\dot{\boldsymbol{\varepsilon}}^{\mathrm{pl}}(\tau) \tag{13}$$

We may now solve the rate problem with the aid of the FEM. Compatibility is written with respect to the rate of the nodal displacements, i.e.,:

$$\dot{\boldsymbol{\varepsilon}}(\tau) = \mathbf{B}\dot{\mathbf{r}}(\tau) \tag{14}$$

Since the residual stresses are self-equilibrated we may have from the PVW:

$$\int_{\mathrm{V}} \delta\dot{\boldsymbol{\varepsilon}}(\tau)^{\mathrm{T}}\dot{\boldsymbol{\rho}}(\tau)\mathrm{d}V = 0 \tag{15}$$

Thus, we end up with solving the following direct stiffness equation with its r.h.s. known:

$$\mathbf{K}\dot{\mathbf{r}}(\tau) = \int \mathbf{B}^{\mathrm{T}}\dot{\boldsymbol{\sigma}}^{\mathrm{el}}(\tau)\mathrm{d}V + \int \mathbf{B}^{\mathrm{T}}\mathbf{D}\dot{\mathbf{e}}^{\theta}(\tau)\mathrm{d}V + \int \mathbf{B}^{\mathrm{T}}\mathbf{D}\dot{\boldsymbol{\varepsilon}}^{\mathrm{pl}}(\tau)\mathrm{d}V \tag{16}$$

With $\dot{\mathbf{r}}(\tau)$ known, we may estimate the values of $\dot{\boldsymbol{\rho}}(\tau)$, using (14) and (13).

Assuming that our structure is made of an elastic–perfectly plastic material, having a yield surface f, and assuming an associated flow rule, the plastic strain rates are given by:

$$\dot{\boldsymbol{\varepsilon}}^{\mathrm{pl}} = \lambda \cdot \frac{\partial f}{\partial \boldsymbol{\sigma}} \tag{17}$$

For stable materials of a convex yield surface [1], it has been proved [33] that a structure will reach, after many cycles of loading, a steady cycle, in which the stresses and the strain rates gradually stabilize and remain unaltered on passing to the next cycle [34]. In such a case, the stresses and the plastic strain rates will become periodic with the same period of the applied loads [35].

Steady state cycles are distinguished by the existence or non-existence of plastic straining inside the cycle. For the former case, from the point of view of kinematics, the plastic strain increment over the cycle constitutes a compatible strain field. Two distinct such cycles [36] may occur, both of which should be avoided, when designing a structure:

(a) The net plastic strain increment is different to zero. Such a cycle, which takes place for relatively high levels of loading, leads the structure to a long-term incremental collapse or ratcheting. Thus, the structure will become unserviceable as the plastic strains will grow bigger from cycle to cycle leading to large displacements.

(b) The net plastic strain increment is equal to zero. The long-term response is reverse plasticity which occurs also for relatively high loading levels and leads to low-cycle fatigue that reduces the working life of a structure or of a component.

For lower levels of cyclic loading, a favorable situation may occur, i.e., a steady cycle where plastic strain rates ($\dot{\boldsymbol{\varepsilon}}^{\mathrm{pl}} = \mathbf{0}$) vanish over the whole body. Thus, despite an initial plastic straining during the transient period, the long-term behavior of the structure becomes purely elastic. This steady state is called elastic shakedown.

The conditions for shakedown have been stated by Melan [2]. The theorem contains the two following statements [34]:

(a) The structure will shake down under a cyclic loading if there exists a time-independent distribution of residual stresses $\bar{\boldsymbol{\rho}}$ such that, under any combination of loads inside prescribed limits, its superposition with the 'elastic' stresses $\boldsymbol{\sigma}^{\mathrm{el}}$, i.e., $\boldsymbol{\sigma}^{\mathrm{el}} + \bar{\boldsymbol{\rho}}$, results in a safe stress state at any point of the structure,

(b) Shakedown never takes place unless a time-independent distribution of residual stresses can be found such that under all the possible load combinations the sum of the residual and 'elastic' stresses constitutes an allowable stress state.

Although originally the theorem of Melan included only mechanical loading, the term 'elastic' refers to stresses generated by either mechanical or thermal load or a combined action of the two. The generalization of Melan's theorem so as to cover thermal cycling was provided by Prager [4].

For a structure subjected to a prescribed cyclic loading program, these statements define the *limit* cycle which is a transition cycle between one with plastic straining and one without plastic straining. It may be proved [34] that the residual stress distribution of this cycle is unique, being independent of the preceding deformation history. The numerical procedure, which will be described below, is exactly a transition process to this cycle.

3 Procedure for shakedown analysis

The approach for the shakedown analysis is based on the RSDM which is a numerical process that provides a cyclic elasto-plastic stress state for a cyclically loaded elasto-plastic structure [32]. The method assumes the decomposition of the residual stresses into Fourier series (e.g., [37]) with respect to the cycle time. Thus, one may write:

$$\boldsymbol{\rho}(\tau) = \frac{1}{2}\mathbf{a}_0 + \sum_{\mathrm{k}=1}^{\infty} \{\cos(2k\pi\tau) \cdot \mathbf{a}_{\mathrm{k}} + \sin(2k\pi\tau) \cdot \mathbf{b}_{\mathrm{k}}\} \tag{18}$$

The coefficients of the series $\mathbf{a}_0$, $\mathbf{a}_{\mathrm{k}}$ and $\mathbf{b}_{\mathrm{k}}$ are calculated through iterations.

The procedure will be termed RSDM-S and is going to be formulated for two-dimensional structures with a von Mises yield surface.

Let us suppose that a structure having thickness d is subjected to a mechanical and a thermal load that vary independent to each other. These loads may have a cyclic variation between a specified maximum and a minimum value just like the cyclic program ($0 \rightarrow P^* \rightarrow (P^*, \theta^*) \rightarrow \theta^* \rightarrow 0$) (Fig. 2a). Without loss of generality, we assume that the minimum values of the two loads are zero with the starred quantities corresponding to the maximum values of the loads. Although the procedure may be applied for more than two loads, for simplicity reasons, a maximum of two loads are considered.

One may obtain a load variation with time by drawing a curve that passes through the limits.

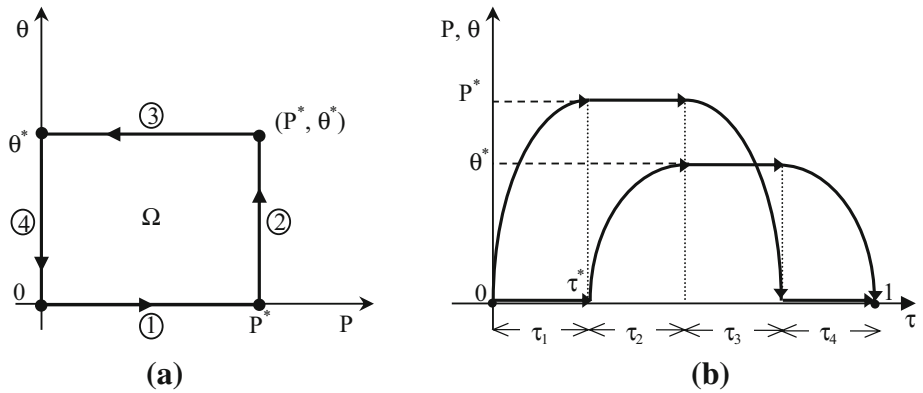

Fig. 2 Individual cyclic loading variation over one time period **a** in load space, **b** in time domain

In the time domain, this cyclic loading may be expressed as:

$$\mathbf{P}(\tau) = \begin{Bmatrix} P(\tau) \\ \theta(\tau) \end{Bmatrix} = \begin{Bmatrix} P^* \cdot \alpha_1(\tau) \\ \theta^* \cdot \alpha_2(\tau) \end{Bmatrix} \tag{19}$$

Indicative variations of the two loads may be seen in Fig. 2b.

Due to the convexity of the yield surface [38] it has been proved that if a given structure shakes down over the path of Fig. 2a that defines the domain Ω then it shakes down over any load path contained within Ω.

Equation (19) converts the problem of a prescribed loading domain to an equivalent prescribed cyclic loading in the time domain. We may expand or contract the loading domain isotropically by multiplying the variation of the loads with a factor γ. Through the proposed iterative procedure, we seek to find the factor γ_{sh} for which the adopted cyclic loading makes the structure shakedown. The procedure that will be presented below will approach this factor by a continuous shrinking of the load domain. Thus, we need to start from a value which is definitely above the shakedown load.

3.1 Evaluation of a starting value for γ

The elastic effective stresses at all the Gauss points (GPs) at τ^* (Fig. 2b) are calculated. This is the cycle time point that one of the loads, for example P, attains its maximum value P^* and the other load θ is zero. Let us suppose that $\min \bar{\sigma}^{\text{el}}(\tau^*)$ is the nonzero minimum of these stresses. The factor

$$\gamma^{(0)} = \frac{\sigma_{\text{Y}}}{\min \bar{\sigma}^{\text{el}}(\tau^*)} \tag{20}$$

where σ_{Y} is the uniaxial yield stress, will constitute a starting loading factor which when multiplying the corresponding loads at τ^* will produce a load which, at least for this cycle time, is far above the shakedown or even the limit load, since all the elements of the structure will be plastic.

3.2 Development of the numerical procedure

As already mentioned for a structure to shakedown, the steady state residual stresses must be constant in time. Since the residual stresses are decomposed in Fourier series [Eq. (18)] the basis of the numerical approach is to lead the coefficients of the trigonometric part of the series a_{k} and b_{k} to zero. The sum of the norms of these terms is used to succeed in this.

Thus, having found an initial solution, we use the RSDM for the factored cyclic loading $\gamma^{(0)} \cdot \mathbf{P}(\tau)$, to produce an initial estimate for $\boldsymbol{\rho}_{(0)}, \mathbf{a}_0^{(0)}, \mathbf{a}_{\text{k}}^{(0)}, \mathbf{b}_{\text{k}}^{(0)}$. Then, we enter the iterative phase, which consists of two iteration loops, one inside the other.

The following iterative steps are then followed:

1. Inside an iteration κ of the outer loop, starting with $\kappa = 1$, the following expressions are calculated in order to find a decreased update $\gamma^{(\kappa)}$ of the loading factor:

$$\varphi\left(\gamma^{(\kappa-1)}\right) = \sum_{\text{k}=1}^{\infty} \left\| \mathbf{a}_{\text{k}}^{(\kappa-1)} \right\| + \sum_{\text{k}=1}^{\infty} \left\| \mathbf{b}_{\text{k}}^{(\kappa-1)} \right\| \tag{21}$$

$$\gamma^{(\kappa)} \cdot P^* = \gamma^{(\kappa-1)} \cdot P^* - \varphi\left(\gamma^{(\kappa-1)}\right) \cdot d \tag{22}$$

   Note that the thickness d is needed to convert stresses to loads

2. The following inequality is checked:

$$\frac{\left|\gamma^{(\kappa)} - \gamma^{(\kappa-1)}\right|}{\gamma^{(\kappa)}} \leq \text{tol} \tag{23}$$

   If ineq. (23) holds, the procedure stops and $\gamma^{(\kappa)} = \gamma^{(\kappa-1)} = \gamma_{\text{sh}}$, otherwise we set

$$\boldsymbol{\rho}_{(\kappa-1)}^{(1)}(\tau) = \boldsymbol{\rho}_{(\kappa-1)}(\tau) \tag{24}$$

3. Using the updated load factor of the outer loop, an inner loop of iterations controlled by μ starts with $\mu = 1$. The following expression, concerning the total stress in the structure, is computed for each cycle point τ and for each GP:

$$\boldsymbol{\sigma}^{(\mu)}(\tau) = \gamma^{(\kappa)}\boldsymbol{\sigma}^{\mathrm{el}}(\tau) + \boldsymbol{\rho}^{(\mu)}_{(\kappa-1)}(\tau) \tag{25}$$

where:

$$\boldsymbol{\sigma}^{\mathrm{el}}(\tau) = \alpha_1(\tau)\boldsymbol{\sigma}^{\mathrm{el}}_{P^*} + \alpha_2(\tau)\boldsymbol{\sigma}^{\mathrm{el}}_{\theta^*} \tag{26}$$

with $\alpha_1(\tau), \alpha_2(\tau)$ the time functions of the loading [Eq. (19)]. Note that $\boldsymbol{\sigma}^{\mathrm{el}}_{P^*}$ and $\boldsymbol{\sigma}^{\mathrm{el}}_{\theta^*}$ are the elastic stresses for P^* and θ^*, respectively.

4. We check whether the effective stress $\bar{\sigma}^{(\mu)}(\tau) > \sigma_{\mathrm{Y}}$; if this does not hold we set $\xi = 0$ otherwise:

$$\xi = \frac{\bar{\sigma}^{(\mu)}(\tau) - \sigma_{\mathrm{Y}}}{\bar{\sigma}^{(\mu)}(\tau)} \Rightarrow \boldsymbol{\sigma}^{(\mu)}_{\mathrm{pl}}(\tau) = \xi \cdot \boldsymbol{\sigma}^{(\mu)}(\tau) \tag{27}$$

This operation is a radial return type rule and may be graphically seen in Fig. 3. For a more detailed discussion the reader is referred to [32].

5. Steps 3 and 4 are repeated for every GP.
6. If we integrate over all GPs, we get:

$$\dot{\mathbf{R}} = \gamma^{(\kappa)}\left\{\dot{\alpha}_1(\tau)\mathbf{R}_{P^*} + \dot{\alpha}_2(\tau)\int_{\mathrm{V}}\mathbf{B}^{\mathrm{T}}\mathbf{D}\mathbf{e}^{\theta^*}\mathrm{d}V\right\} + \int_{\mathrm{V}}\mathbf{B}^{\mathrm{T}}\boldsymbol{\sigma}^{(\mu)}_{\mathrm{pl}}\mathrm{d}V \tag{28}$$

This expression is obtained if we substitute first $\dot{\mathbf{e}}^{\theta} = \dot{\alpha}_2(\tau)\mathbf{e}^{\theta}$, and then Eq. (26), in the expression (16), with $\mathbf{R}_{P^*}$ being the equivalent nodal forces of the elastic FE solution for P^*

7. We find an update for $\dot{\mathbf{r}}^{(\mu)}(\tau)$ by solving Eq. (16).
8. A value for $\dot{\boldsymbol{\rho}}^{(\mu)}(\tau)$ is obtained from Eq. (13), substituting for $\dot{\boldsymbol{\sigma}}^{\mathrm{el}}(\tau) = \gamma^{(\kappa)}\left[\dot{\alpha}_1(\tau)\boldsymbol{\sigma}^{\mathrm{el}}_{P^*} + \dot{\alpha}_2(\tau)\boldsymbol{\sigma}^{\mathrm{el}}_{\theta^*}\right]$ for all the Gauss points.
9. The steps 3–8 are repeated for all the cycle time points.

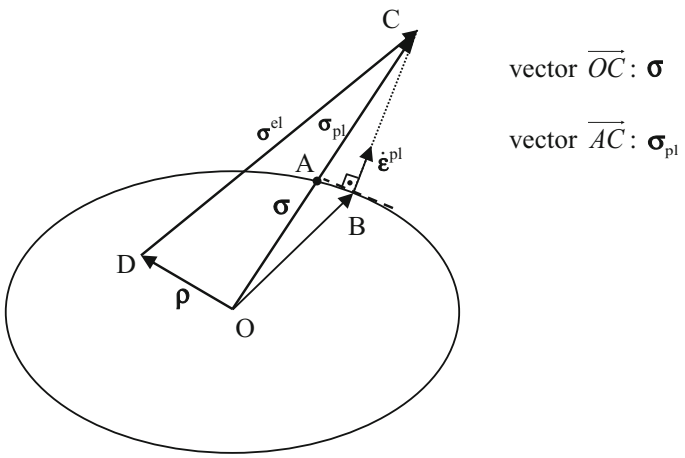

Fig. 3 Von Mises yield surface and radial return type of mapping

10. By performing a numerical time integration over the whole cycle we may obtain an update of the Fourier coefficients [32]:

$$\mathbf{a}_{\mathrm{k}}^{(\mu+1)} = -\frac{1}{k\pi}\int_0^1 \left\{\left[\dot{\boldsymbol{\rho}}^{(\mu)}(\tau)\right](\sin 2k\pi\tau)\right\}\mathrm{d}\tau$$

$$\mathbf{b}_{\mathrm{k}}^{(\mu+1)} = \frac{1}{k\pi}\int_0^1 \left\{\left[\dot{\boldsymbol{\rho}}^{(\mu)}(\tau)\right](\cos 2k\pi\tau)\right\}\mathrm{d}\tau$$

$$\frac{\mathbf{a}_0^{(\mu+1)}}{2} = -\sum_{\mathrm{k}=1}^{\infty}\mathbf{a}_{\mathrm{k}}^{(\mu+1)} + \frac{\mathbf{a}_0^{(\mu)}}{2} + \sum_{\mathrm{k}=1}^{\infty}\mathbf{a}_{\mathrm{k}}^{(\mu)} + \int_0^1 \left[\dot{\boldsymbol{\rho}}^{(\mu)}(\tau)\right]\mathrm{d}\tau \tag{29}$$

11. From the expressions (29), one may get an update for $\boldsymbol{\rho}^{(\mu+1)}(\tau)$ using (18).
12. Next we check whether the values of the residual stresses at the current and at the previous iteration differ within some tolerance at some cycle point, for example at the end of the cycle, i.e.,:

$$\frac{\left\|\boldsymbol{\rho}^{(\mu+1)}(1)\right\|_2 - \left\|\boldsymbol{\rho}^{(\mu)}(1)\right\|_2}{\left\|\boldsymbol{\rho}^{(\mu+1)}(1)\right\|_2} \leq \mathrm{tol} \tag{30}$$

13. In case this does not hold we set $\boldsymbol{\rho}_{(\kappa-1)}^{(\mu+1)}(\tau) = \boldsymbol{\rho}^{(\mu+1)}(\tau)$ and go back to step 3 and start a new iteration of the inner loop; otherwise we set $\boldsymbol{\rho}_{(\kappa)}(\tau) = \boldsymbol{\rho}^{(\mu+1)}(\tau)$ and go back to step 1 and start a new iteration of the outer loop.

Because of Eq. (22), a descending sequence of cyclic solutions is created which ends up with the parameters of the limiting cycle for elastic shakedown. The algorithm is guaranteed to converge monotonically to the solution [39] as the numerical results show that the continuous shrinking of the loading domain produces a strictly descending continuous function, such as φ, which approaches zero, within some tolerance when the shakedown factor γ_{sh} is reached. For accurate results, a value of tol of 10^{-4} proved sufficient. This is equivalent to a tolerance for φ of 10^{-3}.

Thus, the only term that remains in the Fourier series is the constant in time distribution of the residual stresses which is unique for the adopted prescribed loading program.

4 Numerical examples

Two plane stress examples of plate problems were solved following the above procedure. The tolerance adopted, as already mentioned, was 10^{-4}.

4.1 Bree problem

The first example under consideration is the classical Bree plate problem [40] which is a benchmark example for the case of cyclic thermo-mechanical loading. The structure is subjected to an axial stress, constant with time, and a fluctuation of temperature difference $\Delta\theta(\tau)$, assumed to be linearly distributed along the width of the plate (Fig. 4). The plate is assumed homogeneous, isotropic, elastic–perfectly plastic with the following material data: Young's modulus $E = 208\,\mathrm{GPa}$, Poison's ratio $\nu = 0.3$, and yield stress $\sigma_{\mathrm{Y}} = 360\,\mathrm{MPa}$, and the coefficient of thermal expansion is taken as $5 \times 10^{-5}/^{\circ}C$. The same geometrical data to discretize the problem as in [26] are used. The finite element mesh is shown in Fig. 4 and consists of one hundred and twenty, eight-noded, iso-parametric elements with 3×3 Gauss integration points. It is assumed that the plate is constrained from in-plane bending, thus making the problem essentially one- dimensional.

A prescribed loading in the time domain for the temperature may be established with the use of the polynomial time function as shown in Fig. 5. In Fig. 6, one may see the calculated shakedown domain by the RSDM-S i.e., the maximum thermal elastic stress due to the fluctuating temperature σ_{t} plotted versus the axial stress σ_{P} both normalized against the yield stress σ_{Y}. It may be observed that the solution is almost identical with the analytic solution [40].

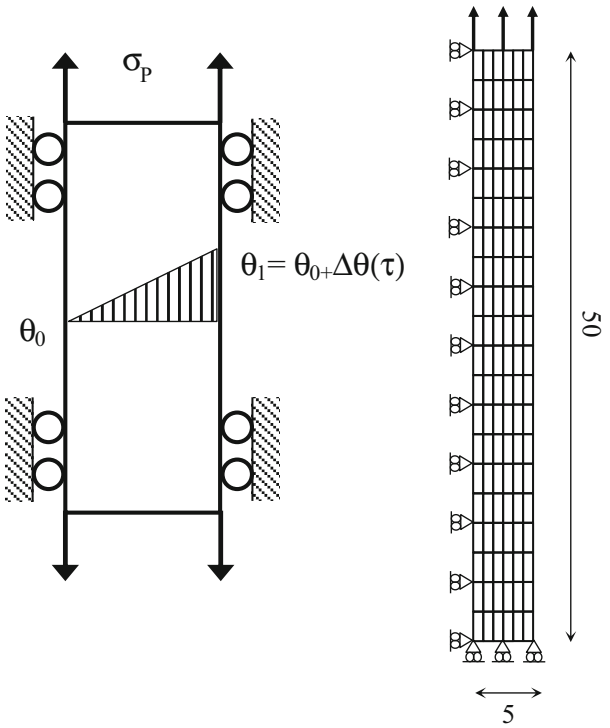

Fig. 4 Geometry, loading and finite element mesh for the Bree problem

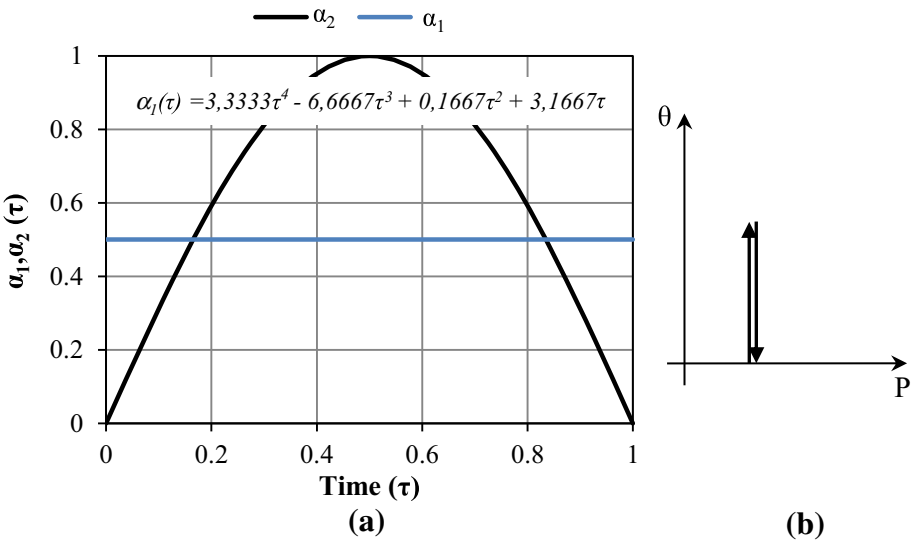

Fig. 5 Cyclic loading variation over one time period in **a** time domain, **b** in load domain

4.2 Square plate with a hole

A second example of application is a square plate with a circular hole at its center (Fig. 7). The plate is assumed homogeneous, isotropic, elastic–perfectly plastic with the same material data as before. The ratio between the diameter D of the hole and the length L of the plate is equal to 0.2. Also the ratio of the thickness d of the plate to its length is equal to 0.05. A case of $L = 20\,\text{cm}$ has been considered. Due to the symmetry of the structure and the loading, only one quarter of the plate is analyzed. The finite element mesh discretization of the plate is also shown in Fig. 7. Ninety-eight, eight-noded, iso-parametric elements with 3×3 Gauss integration points were used.

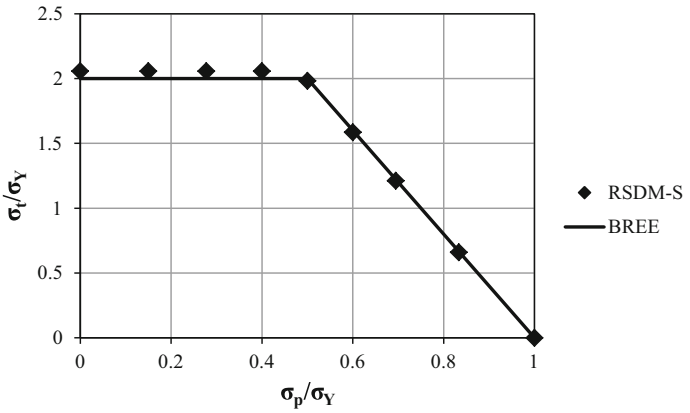

Fig. 6 Shakedown domain produced by the RSDM-S and its comparison with the analytical solution of Bree [40]

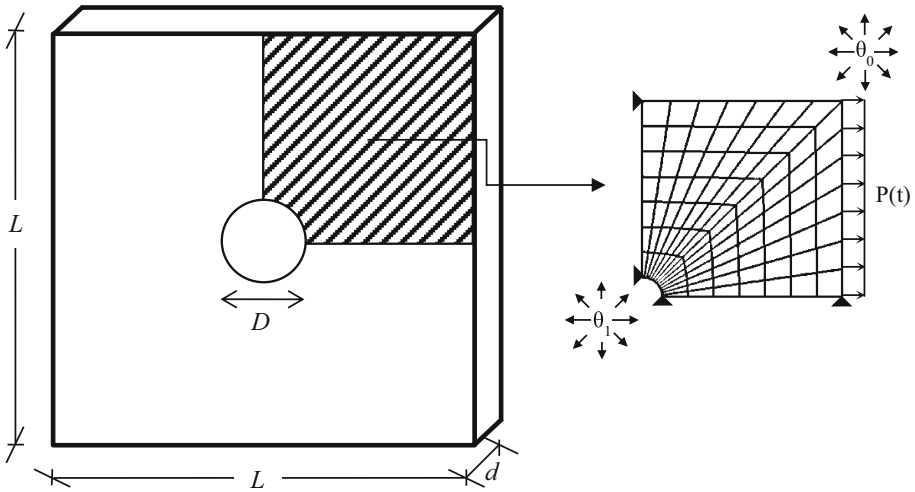

Fig. 7 The geometry of the holed plate subjected to mechanical and thermal loading and its finite element mesh

The plate is subjected to a temperature difference $\Delta\theta$ between the edge of the hole and the edge of the plate, and a uniaxial tension P along the one side of the plate (Fig. 7). The same logarithmic variation of the temperature with radius r as in [31] is used:

$$\theta(r,\tau) = \theta_0 + \Delta\theta(\tau)\ln\left(\frac{5D/2}{r}\right) / \ln(5)$$

The above equation defines the temperature variation inside the plate giving a value of $\theta_1(\tau) = \theta_0 + \Delta\theta(\tau)$ around the edge of the hole ($r = D/2$) and $\theta_1 = \theta_0$ at the outer edges of the plate ($r = 5D/2$). The temperature θ_0 is considered equal to zero, and a coefficient of thermal expansion of $5E-5\,^{\circ}\mathrm{C}^{-1}$ is assumed. In the results, σ_t denotes the maximum effective thermal elastic stress that appears under the fluctuating temperature.

The shakedown domain was calculated for two different load cases of thermo-mechanical loading. A first one assuming constant axial load and variable temperature difference $\Delta\theta(\tau)$ and a second one assuming an independent variation between the axial load and the temperature difference.

4.2.1 Constant axial load P, variable temperature $\Delta\theta(\tau)$

A prescribed loading in the time domain for the temperature may be established with the use of the polynomial time function (Fig. 5), whereas the axial load is considered to be constant with time. In Fig. 8, one may see

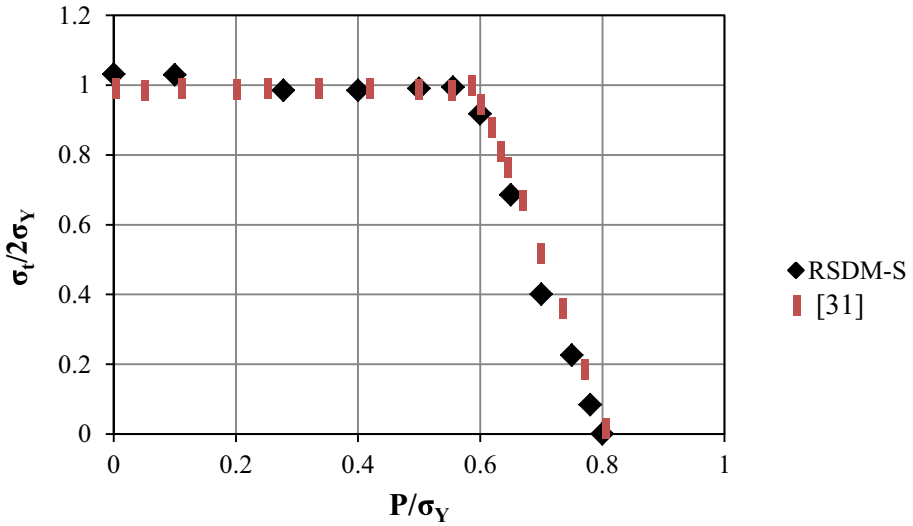

Fig. 8 Shakedown domain produced by the RSDM-S for loading case a (constant mechanical loading)

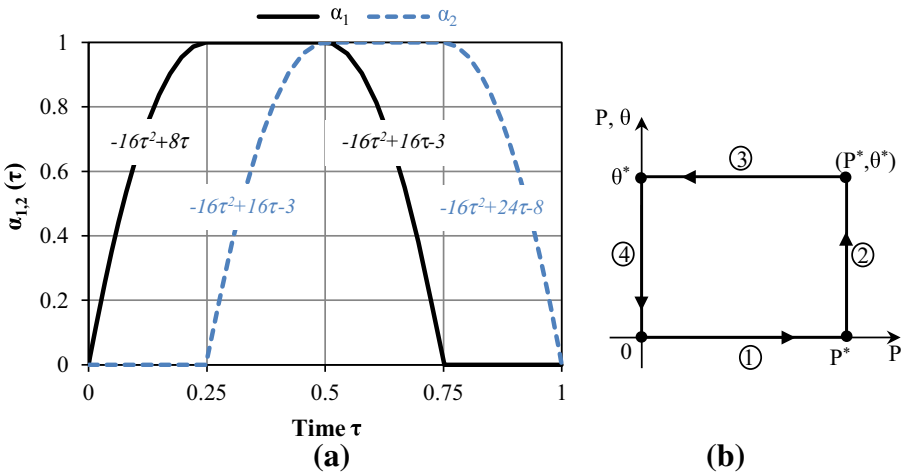

Fig. 9 Independent cyclic loading variation over one time period in **a** time domain, **b** in load domain

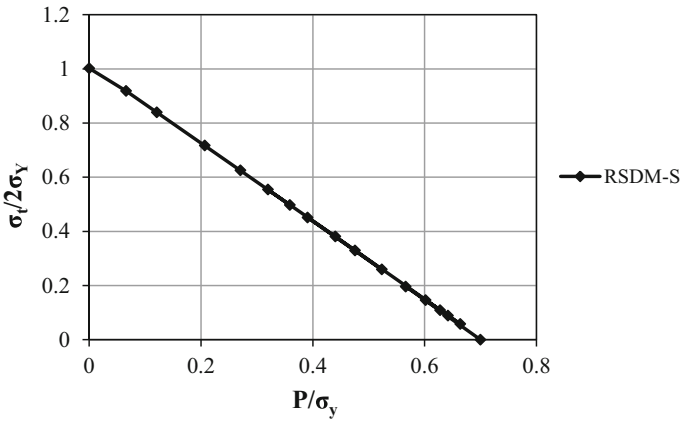

Fig. 10 Shakedown domain produced by the RSDM-S for loading case b (independent load case, rectangular loading domain)

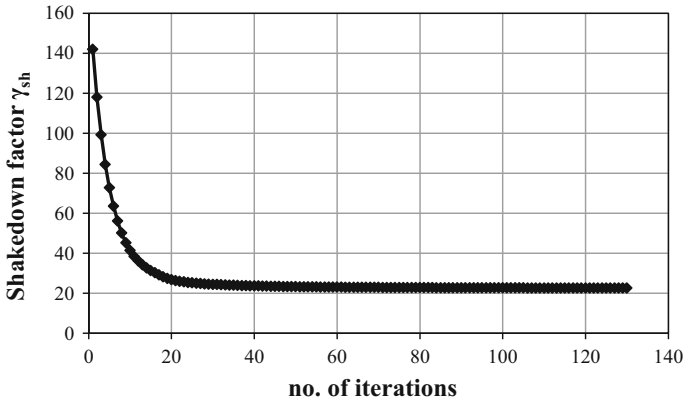

Fig. 11 Typical convergence of the RSDM-S (case of rectangular loading domain)

the results produced by the RSDM-S. It is noted that the temperature axis is normalized against $2\sigma_Y$ as this is the value of σ_t at the reverse plasticity limit [31]. It may be observed that the interaction diagram follows the classic Bree-like shape [40]. A good agreement with existing in the literature results [31] may be seen.

4.2.2 Independent variation of axial load $P(\tau)$, temperature $\Delta\theta(\tau)$

The RSDM-S is used to find the shakedown loading for the rectangular loading domain of Fig. 9b which was discussed before. The time functions of Fig. 9a were used to establish a prescribed cyclic loading that passes through the four vertices of this domain. The computed, by the RSDM-S, shakedown domain is shown in Fig. 10. In Fig. 11, one may see the convergence of the proposed procedure towards the value of the shakedown factor, which is typical for all the cases considered herein.

The developed procedure is computationally efficient as the stiffness matrix of the structure is formed and decomposed only once. Three terms of the Fourier series proved enough to represent the residual stress field.

5 Concluding remarks

A direct method to evaluate the shakedown load of cyclically loaded elasto-plastic structures under thermo-mechanical loading has been presented. The loading domain is first converted into a prescribed loading which is multiplied by a load factor. Then, starting from a factor high above shakedown a descending sequence of loading factors is formed which converges to the parameters of the limit cycle, where the residual stresses are constant in time.

The approach turns out to be simple, numerically stable and efficient and may be implemented in any existing FE code as opposed to MP methods where a special optimization algorithm is also needed to be supplied.

References

1. Drucker, D.C.: A definition of stable inelastic material. ASME J. Appl. Mech. **26**, 101–106 (1959)
2. Melan, E.: Zur Plastizität des räumlichen Kontinuums. Ing. Arch. **9**, 116–126 (1938)
3. Koiter, W.: In: Sneddon, I.N., Hill, R. (eds.) General Theorems for Elastic–Plastic Solids. North-Holland, Amsterdam (1960)
4. Prager, W.: Shakedown in Elastic–Plastic Media Subjected to Cycles of Load and Temperature, Symp. su la Plasticita nella Scienza delle Construzioni, Bologna, pp. 239–244 (1957)
5. Donato, O.: Second shakedown theorem allowing for cycles of both loads and temperature. Rend. Ist. Lombardo Scienza Lettere (A) **104**, 265–277 (1970)
6. Weichert, D.: On the influence of geometrical nonlinearities on the shakedown of elastic–plastic structures. Int. J. Plast. **2**, 135–148 (1986)
7. Pham, D.C.: Shakedown static and kinematic theorems for elastic–plastic limited linear kinematic hardening solids. Eur. J. Mech. A/Solids **24**, 35–45 (2005)
8. Stein, E., Zhang, G., König, J.A.: Shakedown with nonlinear strain-hardening including structural computation using finite element method. Int. J. Plast. **8**, 1–31 (1992)
9. Bousshine, L., Chaaba, A., Saxcé, G.de : A new approach to shakedown analysis for non-standard elastoplastic material by the bipotential. Int. J. Plast. **19**, 583–598 (2003)

10. Polizzotto, C.: Shakedown theorems for elastic–plastic solids in the framework of gradient plasticity. Int. J. Plast. **24**, 218–241 (2008)
11. Borino, G., Polizzotto, C.: Dynamic shakedown of structures with variable appended masses and subjected to repeated excitations. Int. J. Plast. **12**, 215–228 (1996)
12. Maier, G.: Shakedown theory in perfect elastoplasticity with associated and nonassociated flow-laws: a finite element, linear programming approach. Meccanica **4**, 1–11 (1969)
13. Heitzer, M., Staat, M.: Basis reduction technique for limit and shakedown problems. In: Staat, M., Heitzer, M. (eds.) Numerical Methods for Limit and Shakedown Analysis, NIC Series, vol. 15, pp. 1–55 (2003)
14. Zouain, N., Borges, L., Silveira, J.L.: An algorithm for shakedown analysis with nonlinear yield function. Comp. Methods Appl. Mech. Eng. **191**, 263–2481 (2002)
15. Andersen, K.D., Christiansen, E., Overton, M.L.: Computing limit loads by minimizing a sum of norms. SIAM J. Sci. Comput. **19**, 1046–1062 (1998)
16. Bisbos, C.D., Makrodimopoulos, A., Pardalos, P.M.: Second-order cone programming approaches to static shakedown analysis in steel plasticity. Optim. Methods Softw. **20**, 25–52 (2005)
17. Pastor, F., Loute, E.: Solving limit analysis problems: an interior-point method. Commun. Numer. Meth. Eng. **21**, 631–642 (2005)
18. Tran, T.N., Liu, G.R., Nguyen-Xuan, H., Nguyen-Thoi, T.: An edge-based smoothed finite element method for primal-dual shakedown analysis of structures. Int. J. Numer. Meth. Eng. **82**, 917–938 (2010)
19. Simon, J-W., Weichert, D.: Numerical lower bound shakedown analysis of engineering structures. Comp. Methods Appl. Mech. Eng. **200**, 2828–2839 (2011)
20. Garcea, G., Leonetti, L.: A unified mathematical programming formulation of strain driven and interior point algorithms for shakedown and limit analysis. Int. J. Numer. Meth. Eng. **88**, 1085–1111 (2011)
21. Simon, J.-W., Kreimeier, M., Weichert, D.: A selective strategy for shakedown analysis of engineering structures. Int. J. Numer. Meth. Eng. **94**, 985–1014 (2013)
22. Spiliopoulos, K., Weichert, D.: Direct Methods for Limit States in Structures and Materials. Springer, Berlin (2014)
23. Zarka, J., Engel, J.J., Inglebert, G.: On a simplified inelastic analysis of structures, Nucl. Eng. Des. 333–368 (1980)
24. Ponter, A.R.S., Carter, K.F.: Shakedown state simulation techniques based on linear elastic solutions. Comput. Methods Appl. Mech Eng. **140**, 259–279 (1997)
25. Mackenzie, D., Boyle, J.T., Hamilton, R.: The elastic compensation method for limit and shakedown analysis: a review. J. Strain Anal. **35**, 171–188 (2000)
26. Ponter, A.R.S., Engelhardt, M.: Shakedown limits for a general yield condition: implementation and application for a von Mises yield condition. Eur. J. Mech. A/Solids **19**, 423–445 (2000)
27. Chen, H.F., Ponter, A.R.S.: Shakedown and limit analyses for 3-D structures using the linear matching method. Int. J. Press. Vess. Piping **78**, 443–451 (2001)
28. Boulbibane, M., Collins, I.F., Ponter, A.R.S., Weichert, D.: Shakedown of unbound pavements. Road Mat. Pavem. Des. **6**, 81–96 (2005)
29. Boulbibane, M., Ponter, A.R.S.: The linear matching method for the shakedown analysis of geotechnical problems. Int. J. Numer. Anal. Meth. Geomech. **30**, 157–179 (2006)
30. Ponter, A.R.S., Chen, H.: A minimum theorem for cyclic load in excess of shakedown, with application to the evaluation of a ratchet limit. Eur. J. Mech. A/Solids **20**, 539–553 (2001)
31. Chen, H.F., Ponter, A.R.S.: A method for the evaluation of a ratchet limit and the amplitude of plastic strain for bodies subjected to cyclic loading. Eur. J. Mech. A/Solids **20**, 555–571 (2001)
32. Spiliopoulos, K.V., Panagiotou, K.D.: A direct method to predict cyclic steady states of elastoplastic structures. Comp. Methods Appl. Mech. Eng. **223–224**, 186–198 (2012)
33. Frederick, C.O., Armstrong, P.J.: Convergent internal stresses and steady cyclic states of stress. J. Strain Anal. **1**, 154–169 (1966)
34. Gokhfeld, D.A., Cherniavsky, O.F.: Limit Analysis of Structures at Thermal Cycling. Sijthoff & Noordhoff, Alphena (1980)
35. Polizzotto, C.: Variational methods for the steady state response of elastic–plastic solids subjected to cyclic loads. Int. J. Solids Struct. **40**, 2673–2697 (2003)
36. König, J.A.: Shakedown of Elastic–Plastic Structures. Elsevier, Amsterdam (1987)
37. Tolstov, G.P.: Fourier Series. Dover, New York (1962)
38. König, J.A., Kleiber, M.: On a new method of shakedown analysis. Bull. Acad. Polon. Sci. Ser. Sci. Tech. **26**, 165–171 (1978)
39. Luenberger, D.G., Ye, Y.: Linear and Nonlinear Programming. Springer, New York (2008)
40. Bree, J.: Elastic–plastic behaviour of thin tubes subjected to internal pressure and intermittent high-heat fluxes with application to fast-nuclear-reactor fuel elements. J. Strain Anal. **2**, 226–238 (1967)